Memorias del XX Congreso Latinoamericano de Control Automático (CLCA 2025)
13-17 de Octubre, 2025. Cancún, Quintana Roo, México

Flocking control for a group of wheeled mobile robots free of linear velocity measurements ⋆

Carlos Montañez-Molina * **Javier Pliego-Jiménez** *,** **César Cruz-Hernández** *

* *Departamento de Electrónica y Telecomunicaciones, División de Física Aplicada, CICESE Carretera Ensenada-Tijuana, 3918 Ensenada, B.C. México (e-mail: carlosm@cicese.edu.mx, jpliego@cicese.edu.mx, ccruz@cicese.mx).*
** *Programa Investigadores por México, SECIHTI, Ciudad de México, México (e-mail: jpliego@cicese.edu.mx)*

Abstract: This research proposes a control algorithm that allows a group of wheeled mobile robots to emulate the flocking behavior. The controller is designed in such a manner that linear velocity measurements are not necessary either locally or in the exchange of information between the group members. Given that in real life it is possible that not all the members of the group to have knowledge of the desired flocking velocity, we propose a distributed observer. Moreover, the proposed flocking controller works for either undirectional or bidirectional communication topologies. To analyze the stability of the flocking algorithm and distributed observer, we employ tools from linear systems theory. To demonstrate the correct functioning of the control law, experimental tests are shown.

Keywords: Flocking, mobile robot, control algorithm, graph theory, velocity tracking.

1. INTRODUCTION

In recent years, researchers and engineers in the area of automatic control and robotics have focused on studying the collective behaviors observed in nature, such as consensus, formation and flocking, to mention a few. The interest in achieving collective behaviors in robotic swarms is motivated by the fact that a group of robots can perform more complicated tasks than a single robot. Besides, using multiple robots can reduce the operation time and maintenance costs. Some tasks that a group of robots can perform are search, surveillance, area mapping, object transportation, to name a few.

In the works reported by (Ren, 2008; Hu and Lin, 2010; Abdessameud and Tayebi, 2013) and (Rojo et al., 2019), the problem of consensus is addressed. Ren (2008) proposes several control algorithms with different properties to tackle the consensus problem. Among these consensus controllers, we can find, for example, a control law with bounded input, a controller free of relative velocity measurements and a control law for velocity tracking. Hu and Lin (2010) consider the case of time delay in the communication. Abdessameud and Tayebi (2013) propose control algorithms with input saturation, the authors also consider the case in which the velocities of the agents are not available for feedback. Rojo et al. (2019) propose to include a trajectory tracking term in the consensus protocol to avoid collisions between the agents.

⋆ This work was supported by SECIHTI Ciencia Básica under grant A1-S-31628.

The problem of formation is studied in the following works. Abdessameud and Tayebi (2009) designed a controller that achieves that a group of aerial vehicles replicate the behavior of formation while they track a desired trajectory. Bazoula and Nemra (2013) propose a control law that allows to the agents of the group to adopt the graph form used for the communication. In (Han et al., 2016; Zhao and Zelazo, 2017) the problem of time varying formations is analyzed, the difference between the first and second works is the type of graph employing for the communication, Han et al. (2016) use directed graph while Zhao and Zelazo (2017) consider undirected connected graph.

On the other hand, the design of control laws to emulate flocking behavior is studied in (Moshtagh et al., 2005), where the authors propose control laws for nonholonomic agents in two and three dimensions, it is important to mention that the agents achieve the flocking behavior even when the communication topologies are time varying. Shi et al. (2009); Gao et al. (2017); Zhao et al. (2017) use the leader-follower strategy to emulate the behavior under study. The authors present numerical simulations to validate the performance of the controller. In contrast to (Shi et al., 2009; Gao et al., 2017),(Zhao et al., 2017) designed a control law for nonlinear systems with nonholonomic constraints. Ning et al. (2018) designed a flocking control law for agents with double integrator dynamic based in interaction rules of acute angle. The authors also include in their controller a term to avoid collision. The control algorithm proposed in (Jian et al., 2018), allows that a group of quadrotors emulate the behavior of flocking, to validate the performance of the controller numerical

https://doi.org/10.58571/CNCA.AMCA.2025.064

results are presented. In contrast with the above work, Saif et al. (2019) present experimental results. On the other hand, to minimize the steady state error caused by unmodeled dynamics Saif et al. (2019) include an integral term in the control algorithm. In (Cheng and Wang, 2020) the problem of flocking is dealt as an optimization problem, the proposed control was designed used potential functions, to validate the control performance Cheng and Wang (2020) have made experimental tests employ a group of differential mobile robots. The case in which the desired velocity is just known by some member of the group is tackled in (Khaledyan et al., 2020), to solve the problem the authors designed a distributed observer. In (Pliego et al., 2023; Cetina et al., 2025), to solve the problem of flocking the authors exploit the cascade structure of the kinematic model of the differential mobile robot, to demonstrate the performance of control laws experimental test are shown.

In this research, we address the problem of flocking for robots with nonholonomic constraints, the proposed controller is free of linear velocity measurements, which is convenient in a practical case, since these measurements are not always available. Moreover, given that an observer is not required the calculations are simplified. Unlike (Pliego et al., 2023), the proposed flocking controller works for either undirected or directed communication topologies. Besides, a distributed observer is proposed to overcome the case in which not all the agents know the desired velocity. The stability of the closed-loop system is exponential and asymptotic. To validate the theory we show experimental results.

2. PRELIMINARIES

2.1 Graph theory

Let $\mathcal{G} = (\mathcal{N}, \mathcal{E})$ be a graph where $\mathcal{N}$ is the set of nodes (agents or robots) and $\mathcal{E}$ is the set of edges $\mathcal{E} \in \mathcal{N} \times \mathcal{N}$. A graph is called directed, if its set of edges is order pair of $\mathcal{N}$ and undirected, if the set of edges is unordered pair of $\mathcal{N}$, in the case of a directed graph the information flows only in one direction while in an undirected graph the information flow is bidirectional. From graph theory is well known that a graph can be represented mathematically by matrices.

The adjacency matrix $\boldsymbol{A} = [a_{ij}] \in \Re^{N\times N}$ for a directed graph is given by

$$a_{ij} = \begin{cases} 1 & j \in \mathcal{N}_i \\ 0 & \text{otherwise} \end{cases}$$

where $\mathcal{N}_i$ is the set of neighbors that transmit information to the agent i, N is the agents number, for an undirected graph $\boldsymbol{A}$ is calculated by

$$a_{ij} = \begin{cases} 1 & \text{if}(i,j) \in \mathcal{E} \\ 0 & \text{otherwise} \end{cases}.$$

The degree matrix $\boldsymbol{D} \in \Re^{N\times N}$ is a diagonal matrix and its components are given by

$$d_{ij} = \begin{cases} \sum_{i=1}^{N} d_i & \text{if } i = j \\ 0 & \text{Otherwise} \end{cases}$$

where d_{ij} are the components of $\boldsymbol{D}$ and d_i is the number of nodes that are adjacents to node i.

The Laplacian matrix $\boldsymbol{L}$ of a directed or an undirected graph is given by

$$\boldsymbol{L} = \boldsymbol{D} - \boldsymbol{A},$$

the Laplacian matrix from an undirected graph is symmetric, for a directed graph the above is no always fulfilled, the matrix $\boldsymbol{L}$ from an undirected or a directed graph has at least one eigenvalue equal to zero, in the case of undirected graph the rest of them are reals and positives, the nonzero eigenvalues of a directed graph can be complex with real part positive, the eigenvalue $\lambda = 0$ of $\boldsymbol{L}$ has associated the eigenvector $\boldsymbol{1}_N = [1 \cdots 1]^\top \in \Re^N$, hence, it is easy to proof that $\boldsymbol{L}\boldsymbol{1}_N = \boldsymbol{0}$, if the eigenvalue $\lambda = 0$ has algebraic multiplicity equal to one allows to say that an undirected graph is connected or that a directed graph is strongly connected (Ren et al., 2007).

2.2 Problem statement

In this work, we aim to emulate the flocking behavior, according to the established for Craig Reynolds (1998), so that the flocking behavior to exist, the members of the group have to obey the following rules: cohesion, alignment and separation. To achieve the above in this document the control objective is defined as

$$\lim_{t\to\infty} \boldsymbol{p}_{ij}(t) - \boldsymbol{\delta}_{ij} = \boldsymbol{0}, \ \lim_{t\to\infty} \boldsymbol{v}_i(t) = \boldsymbol{v}^d(t) \ \ \forall i, j \in \mathcal{N}, \quad (1)$$

where $\boldsymbol{p}_{ij}(t) = \boldsymbol{p}_i(t) - \boldsymbol{p}_j(t) \in \Re^2$ is the relative position, $\boldsymbol{v}^d \in \Re^2$ is the desired velocity of the group and $\boldsymbol{\delta}_{ij} = \boldsymbol{\delta}_i - \boldsymbol{\delta}_j \in \Re^2$ is a constant vector that defines the geometry of the formation.

2.3 Mathematical model of the differential mobile robot

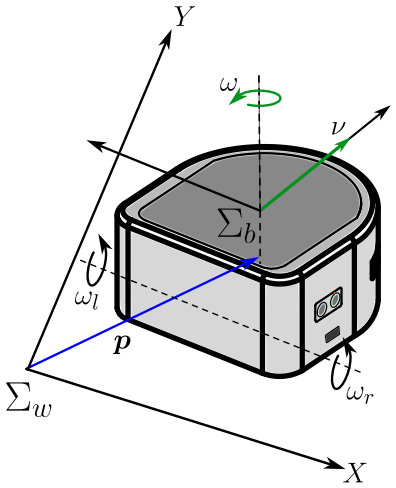

Fig. 1. Differential mobile robot, where ω_l and ω_r are the angular velocity of the wheels

The kinematic model that describes the translation motion and attitude of a differential mobile robot (see Figure 1) is given by

$$\boldsymbol{v} = \nu \boldsymbol{R}\boldsymbol{e}_1 \quad (2a)$$

$$\dot{\boldsymbol{R}} = \omega \boldsymbol{R}\boldsymbol{S}, \quad (2b)$$

where $\boldsymbol{p} \in \Re^2$ is the position vector that goes of the inertial reference frame Σ_w to the body fixed frame Σ_b, $\boldsymbol{v} = \dot{\boldsymbol{p}}$,

 https://doi.org/10.58571/CNCA.AMCA.2025.064

$\nu \in \Re$ is the velocity magnitude and $\omega \in \Re$ is the angular velocity, both are the control inputs, $\boldsymbol{e}_1 = [1\ 0]^\top$ is the unit vector in the axis x, $\boldsymbol{R} \in SO(2)$ is the rotation matrix given by $\boldsymbol{R} = \cos(\theta)\boldsymbol{I} + \sin(\theta)\boldsymbol{S}$ where θ is the stering angle. On the other hand, $\boldsymbol{S} \in \mathfrak{so}(2)$ is the Skew-symmetric matrix represented by $\boldsymbol{S} = [\boldsymbol{e}_2\ -\boldsymbol{e}_1]$, where $\boldsymbol{e}_2 = [0\ 1]^\top$ is the unit vector in the axis y.

3. CONTROL ALGORITHMS

3.1 Velocity control algorithm

Before presenting the proposed flocking control algorithm, we first designed a control algorithm for velocity tracking, which is based on the dynamic feedback linearization technique (Oriolo et al., 2002). To begin with the design of the velocity control algorithm, the term $\lambda\boldsymbol{v}$ (with $\lambda > 0$) is added in the left and right hand sides of the first derivative of the equation (2a) resulting in

$$\dot{\boldsymbol{v}} + \lambda\boldsymbol{v} = \dot{\nu}\boldsymbol{R}\boldsymbol{e}_1 + \nu\dot{\boldsymbol{R}}\boldsymbol{e}_1 + \lambda\boldsymbol{v}, \tag{3}$$

by using the property $\boldsymbol{S}\boldsymbol{R} = \boldsymbol{R}\boldsymbol{S}$ and carrying out some operations the equation (3) is rewritten as

$$\dot{\boldsymbol{v}} + \lambda\boldsymbol{v} = \boldsymbol{R}\begin{bmatrix} \dot{\nu} + \lambda\nu \\ \nu\omega \end{bmatrix} = \boldsymbol{u}, \tag{4}$$

where $\boldsymbol{u}$ is a new auxiliary control input which is designed afterwards. From (4), the control inputs ω and ν can be obtained as follows

$$\begin{bmatrix} \dot{\nu} + \lambda\nu \\ \nu\omega \end{bmatrix} = \boldsymbol{R}^\top\boldsymbol{u} \quad \Longrightarrow \quad \begin{array}{l} \dot{\nu} = -\lambda\nu + \boldsymbol{u}^\top\boldsymbol{R}\boldsymbol{e}_1 \\ \omega = \dfrac{\boldsymbol{u}^\top\boldsymbol{R}\boldsymbol{e}_2}{\nu} \end{array},$$

the control input ν is obtained as the solution of $\dot{\nu} = -\lambda\nu + \boldsymbol{u}^\top\boldsymbol{R}\boldsymbol{e}_1$ as long as $\nu(0) \neq 0$ to avoid an indetermination in the control input ω, for further information about the controller can be consulted the document (Montañez et al., 2023)

3.2 Flocking control algorithm

Taking inspiration from (Montañez et al., 2022) and considering the equation (4) is obtained

$$\dot{\boldsymbol{p}}_i = \boldsymbol{\vartheta}_i + \tilde{\boldsymbol{v}}_i \tag{5a}$$

$$\dot{\tilde{\boldsymbol{v}}}_i = -\lambda_i\boldsymbol{v}_i - \dot{\boldsymbol{\vartheta}}_i + \boldsymbol{u}_i \text{ with } i = 1, ..., N, \tag{5b}$$

where $\tilde{\boldsymbol{v}}_i = \boldsymbol{v}_i - \boldsymbol{\vartheta}_i \in \Re^2$ is the velocity error and $\boldsymbol{\vartheta}_i \in \Re^2$ is a virtual input, for its design it is made use of the error variable

$$\boldsymbol{r}_i = \boldsymbol{p}_i - \boldsymbol{p}^{\mathrm{d}} - \boldsymbol{\delta}_i - \boldsymbol{\varphi}_i \tag{6}$$

where $\boldsymbol{\varphi}_i \in \Re^2$ is an auxiliary variable used to avoid employing the velocity measurements of each agent in the exchange of information. To achieve formation it is desirable that the dynamics of $\boldsymbol{r}_i$ to have the following form

$$\dot{\boldsymbol{r}}_i = -c\sum_{j=1}^{N} a_{ij}\boldsymbol{r}_{ij}, \tag{7}$$

where $c > 0$ is the coupling gain, $\boldsymbol{r}_{ij} = \boldsymbol{p}_{ij} - \boldsymbol{\delta}_{ij} - \boldsymbol{\varphi}_{ij}$ and $\boldsymbol{\varphi}_{ij} = \boldsymbol{\varphi}_i - \boldsymbol{\varphi}_j$. Differentiating (6) and equating it with (7), and considering (5b) when performing some operations, the proposed flocking control law is given by

$$\boldsymbol{\vartheta}_i = \boldsymbol{v}^{\mathrm{d}} - k_{\varphi i}\boldsymbol{\varphi}_i \tag{8a}$$

$$\dot{\boldsymbol{\varphi}} = -k_{\varphi i}\boldsymbol{\varphi}_i + c\sum_{j=1}^{N} a_{ij}\boldsymbol{r}_{ij} \tag{8b}$$

$$\boldsymbol{u}_i = \dot{\boldsymbol{\vartheta}}_i + \lambda_i\boldsymbol{\vartheta}_i, \tag{8c}$$

where λ_i and $k_{\varphi i}$ are positive gains, $\boldsymbol{\varphi}_i$ is obtained as solution of (8b). It is important to emphasize that the controller proposed is velocity-free both when exchanging information among agents as when making velocity tracking, since to carry out velocity tracking the controller just requires the desired velocity profile and its derivatives.

Given that in nature not all the agents of the group know the desired velocity profile, we proposed a distributed observer to tackle the problem. The structure of the observer is given by

$$\dot{\hat{\boldsymbol{v}}}_i^{\mathrm{d}} = -\mu\left(\sum_{j=i}^{N} a_{ij}\hat{\boldsymbol{v}}_{ij}^{\mathrm{d}} + b_i(\hat{\boldsymbol{v}}_i^{\mathrm{d}} - \boldsymbol{v}^{\mathrm{d}})\right), \tag{9}$$

where $\mu > 0$ is a gain, $\hat{\boldsymbol{v}}_i^{\mathrm{d}} \in \Re^2$ is an estimation of $\boldsymbol{v}^{\mathrm{d}}$, $\hat{\boldsymbol{v}}_{ij}^{\mathrm{d}} = \hat{\boldsymbol{v}}_i^{\mathrm{d}} - \hat{\boldsymbol{v}}_j^{\mathrm{d}} \in \Re^2$ and $b_i \in \Re$ indicates which member of the group know the desired velocity profile and it is defined as

$$b_i = \begin{cases} 1 & \text{if } i \in \mathcal{N}^{\mathrm{d}} \\ 0 & \text{otherwise} \end{cases},$$

$\mathcal{N}^{\mathrm{d}} \subset \mathcal{N}$ is the subset of all the agents that know $\boldsymbol{v}^{\mathrm{d}}$, since at least one agent knows $\boldsymbol{v}^{\mathrm{d}}$ is possible estimate it for the agent $i \notin \mathcal{N}^{\mathrm{d}}$.

Proposition 1. Assume that $\mathcal{G}$ is undirected (connected) or directed (strongly connected) and $\dot{\boldsymbol{v}}^{\mathrm{d}}(t) \to 0$ as $t \to \infty$ then, the distributed observer (9) guarantees that $\hat{\boldsymbol{v}}_i^{\mathrm{d}}(t) \to \boldsymbol{v}^{\mathrm{d}}(t)$ as $t \to \infty$ for all $i \in \mathcal{N}$.

Proof. To prove that $\hat{\boldsymbol{v}}_i^{\mathrm{d}}(t) \to \boldsymbol{v}^{\mathrm{d}}(t)$ as $t \to \infty$, we define the following estimation error $\bar{\boldsymbol{v}}_i^{\mathrm{d}} = \hat{\boldsymbol{v}}_i^{\mathrm{d}} - \boldsymbol{v}^{\mathrm{d}}$, getting its first time derivative and using the Kronecker product $\otimes$, the error dynamics $\bar{\boldsymbol{v}}_i^{\mathrm{d}}$ in compact form are given by

$$\begin{aligned} \dot{\bar{\boldsymbol{v}}}_i^{\mathrm{d}} &= -\mu(\boldsymbol{L} \otimes \boldsymbol{I}_2)\bar{\boldsymbol{v}}^{\mathrm{d}} - \mu(\bar{\boldsymbol{D}} \otimes \boldsymbol{I}_2)\bar{\boldsymbol{v}}^{\mathrm{d}} - \boldsymbol{1}_N \otimes \dot{\boldsymbol{v}}^{\mathrm{d}} \\ &= -\mu(\boldsymbol{M} \otimes \boldsymbol{I}_2)\bar{\boldsymbol{v}}^{\mathrm{d}} - \boldsymbol{1}_N \otimes \dot{\boldsymbol{v}}^{\mathrm{d}} \end{aligned} \tag{10}$$

where $\bar{\boldsymbol{v}}_i^{\mathrm{d}} - \bar{\boldsymbol{v}}_j^{\mathrm{d}} = \hat{\boldsymbol{v}}_i^{\mathrm{d}} - \hat{\boldsymbol{v}}_j^{\mathrm{d}}$ has been used, $\boldsymbol{I}_2 \in \Re^{2\times 2}$ is the identity matrix, $\bar{\boldsymbol{v}}^{\mathrm{d}} = [(\bar{\boldsymbol{v}}_1^{\mathrm{d}})^\top\ \cdots\ (\bar{\boldsymbol{v}}_N^{\mathrm{d}})^\top]^\top \in \Re^{2N}$, $\bar{\boldsymbol{D}} = \mathrm{diag}\{b_1\ \cdots\ b_N\} \in \Re^{N\times N}$ and $\boldsymbol{M} = \boldsymbol{L} + \bar{\boldsymbol{D}} \in \Re^{N\times N}$. Since $\mathcal{G}$ has been supposed directed (strongly connected) or undirected (connected), the eigenvalues of $\boldsymbol{M}$ are strictly positives (Hong et al., 2006), hence, the matrix $-\mu(\boldsymbol{M} \otimes \boldsymbol{I}_2)$ is Hurwitz. According to (Hale, 2009) if $\dot{\boldsymbol{v}}^{\mathrm{d}}(t) \to \boldsymbol{0}$ as $t \to \infty$, we concluded that $\lim_{t\to\infty} \bar{\boldsymbol{v}}^{\mathrm{d}}(t) = \boldsymbol{0}$ and it is confirmed that $\hat{\boldsymbol{v}}_i^{\mathrm{d}}(t) \to \boldsymbol{v}^{\mathrm{d}}(t)$. ■

Considering the equation (5) the time derivative of (6), (8), the Kronecker product and the expression (10), the closed-loop dynamics in compact form are given by

$$\dot{\boldsymbol{\varphi}} = -(\boldsymbol{K} \otimes \boldsymbol{I}_2)\boldsymbol{\varphi} + c(\boldsymbol{L} \otimes \boldsymbol{I}_2)\boldsymbol{r} \tag{11a}$$

$$\dot{\boldsymbol{r}} = -(\boldsymbol{L} \otimes \boldsymbol{I}_2)\boldsymbol{r} + \tilde{\boldsymbol{v}} + \bar{\boldsymbol{v}}^{\mathrm{d}} \tag{11b}$$

$$\dot{\tilde{\boldsymbol{v}}} = -(\boldsymbol{\Lambda} \otimes \boldsymbol{I}_2)\tilde{\boldsymbol{v}} \tag{11c}$$

$$\dot{\bar{\boldsymbol{v}}}^{\mathrm{d}} = -\mu(\boldsymbol{M} \otimes \boldsymbol{I}_2)\bar{\boldsymbol{v}}^{\mathrm{d}} - \boldsymbol{1}_N \otimes \dot{\boldsymbol{v}}^{\mathrm{d}}, \tag{11d}$$

 https://doi.org/10.58571/CNCA.AMCA.2025.064

where $\boldsymbol{\varphi} = [\boldsymbol{\varphi}_1^\top; \cdots \ \boldsymbol{\varphi}_N^\top]^\top \in \Re^{2N}$, $\boldsymbol{r} = [\boldsymbol{r}_1^\top; \cdots \ \boldsymbol{r}_N^\top]^\top \in \Re^{2N}$ and $\tilde{\boldsymbol{v}} = [\tilde{\boldsymbol{v}}_1^\top; \cdots \ \tilde{\boldsymbol{v}}_N^\top]^\top \in \Re^{2N}$, $\boldsymbol{K} = \text{diag}\{k_{\varphi 1} \ \cdots \ k_{\varphi N}\}$ and $\boldsymbol{\Lambda} = \text{diag}\{\lambda_1 \ \cdots \ \lambda_N\}$.

Proposition 2. The closed-loop (11) assuming that $\dot{\boldsymbol{v}}^{\text{d}}(t) = \boldsymbol{0}$ or that $\dot{\boldsymbol{v}}^{\text{d}}(t) \to \boldsymbol{0}$ as $t \to \infty$ has as equilibrium point exponentially stable $(\boldsymbol{\varphi}, \boldsymbol{r}, \tilde{\boldsymbol{v}}, \bar{\boldsymbol{v}}^{\text{d}}) = (\boldsymbol{0}, \boldsymbol{1}_N \otimes r^*, \boldsymbol{0}, \boldsymbol{0})$.

Proof. To analyze the stability of the equilibrium point, we make change of coordinates (Nuño et al., 2011)

$$\boldsymbol{q} = (\boldsymbol{Q} \otimes \boldsymbol{I}_n)\boldsymbol{r}, \tag{12}$$

where n is the state dimension, $\boldsymbol{Q} \in \Re^{N-1 \times N}$ is given by

$$\boldsymbol{Q} = \begin{bmatrix} -1+(N-1)\chi & 1-\chi & -\chi & \cdots & -\chi \\ -1+(N-1)\chi & -\chi & 1-\chi & \ddots & \vdots \\ \vdots & \vdots & \ddots & \ddots & -\chi \\ -1+(N-1)\chi & -\chi & \cdots & -\chi & 1-\chi \end{bmatrix} \tag{13}$$

with $\chi = (N - \sqrt{N})/N(N-1)$.

According to (Scardovi et al., 2010), (13) presents the following properties

$$\boldsymbol{Q}\boldsymbol{1}_N = \boldsymbol{0}, \boldsymbol{Q}\boldsymbol{Q}^\top = \boldsymbol{I}_{N-1}, \boldsymbol{Q}^\top\boldsymbol{Q} = \boldsymbol{I}_N - \frac{1}{N}\boldsymbol{1}_N\boldsymbol{1}_N^\top, \tag{14}$$

hence, it follows that

$$\boldsymbol{q} = (\boldsymbol{Q} \otimes \boldsymbol{I}_n)\,\boldsymbol{r} = \boldsymbol{0} \Longrightarrow \boldsymbol{r} = \boldsymbol{1}_N \otimes \boldsymbol{r}^*. \tag{15}$$

Then by considering the change of coordinates and taking account (14) the closed-loop dynamics can be rewritten as

$$\dot{\boldsymbol{\xi}} = \boldsymbol{A}\boldsymbol{\xi} + \boldsymbol{B}(\boldsymbol{1}_N \otimes \dot{\boldsymbol{v}}^{\text{d}}) \tag{16}$$

where $\boldsymbol{\xi} = [\boldsymbol{\varphi}^\top \ \boldsymbol{q}^\top \ \tilde{\boldsymbol{v}}^\top \ (\bar{\boldsymbol{v}}^{\text{d}})^\top]^\top \in \Re^{2(4N-1)}$, the matrix $\boldsymbol{A}$ and $\boldsymbol{B}$ are defined respectively as

$$\boldsymbol{A} = \begin{bmatrix} -(\boldsymbol{K} \otimes \boldsymbol{I}_2) & (\boldsymbol{H}_1 \otimes \boldsymbol{I}_2) & \boldsymbol{O} & \boldsymbol{O} \\ \boldsymbol{O} & -(\boldsymbol{H}_2 \otimes \boldsymbol{I}_2) & (\boldsymbol{Q} \otimes \boldsymbol{I}_2) & (\boldsymbol{Q} \otimes \boldsymbol{I}_2) \\ \boldsymbol{O} & \boldsymbol{O} & -(\boldsymbol{\Lambda} \otimes \boldsymbol{I}_2) & \boldsymbol{O} \\ \boldsymbol{O} & \boldsymbol{O} & \boldsymbol{O} & -\mu(\boldsymbol{M} \otimes \boldsymbol{I}_2) \end{bmatrix},$$

$$\boldsymbol{B} = [\boldsymbol{O} \ \boldsymbol{O} \ \boldsymbol{O} \ \boldsymbol{I}_{2N}]^\top \in \Re^{2(4N-1)\times 2N},$$

where $\boldsymbol{H}_1 = c\boldsymbol{L}\boldsymbol{Q}^\top$, $\boldsymbol{H}_2 = c\boldsymbol{Q}\boldsymbol{L}\boldsymbol{Q}^\top$ and $\boldsymbol{O}$ are matrices of adequate dimensions composed by zeros. Given that $\boldsymbol{A}$ is an upper triangular block matrix and the matrices in its diagonal are Hurwitz, then $\boldsymbol{A}$ is also Hurwitz, recall that $\dot{\boldsymbol{v}}^{\text{d}}$ has to be zero or has to tend to zero (16) is a linear system with equilibrium point exponentially stable, with this result is confirmed that $\boldsymbol{\varphi}_{ij}(t) \to \boldsymbol{0}$ and it is also verified the shown in (15), this implies that $\boldsymbol{r}_i(t) \to \boldsymbol{r}^*$, $\boldsymbol{r}_{ij}(t) \to \boldsymbol{0}$, therefore $\boldsymbol{p}_{ij} - \boldsymbol{\delta}_{ij} = \boldsymbol{r}_{ij} - \boldsymbol{\varphi}_{ij} \to \boldsymbol{0}$. The analysis of stability also confirmed that $\boldsymbol{v}_i(t) \to \hat{\boldsymbol{v}}_i^{\text{d}} \to \boldsymbol{v}_i^{\text{d}}(t)$ as $t \to \infty$, then, the control objective is achieved in the sense of (1) and of $\bar{\boldsymbol{v}}_i^{\text{d}}(t) = \boldsymbol{0}$ as $t \to \infty$.

4. EXPERIMENTAL RESULTS

To validate the theory shown in this document, we have carried out experimental tests, to get the results four differential mobile robots known as Khepera III have been using, this robot is equipped with a DsPiC 30F5011 processor, a RAM memory of 4 KB, eleven infrared sensors, five ultrasonic sensors, two DC motors and one battery of lithium polymer. To measure the position and attitude of the robots six OptiTrack cameras have been employed. The programming of the control algorithm was made in the software Matlab using a sample time of 0.01 [s].

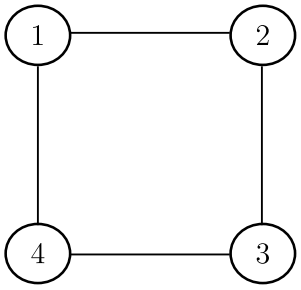

Fig. 2. Undirected graph in ring configuration

The graph used to communicate to each member of the group is depicted in Figure 2. The desired velocity profile is given by

$$\boldsymbol{v}^{\text{d}} = \begin{bmatrix} 0.035 - 0.015(\tanh(t-20) - \tanh(t-35)) \\ -0.015(\tanh(t-20) - \tanh(t-35)) \end{bmatrix} \text{[m/s]},$$

in this experiment is proposed that just the first robot of the group has knowledge of $\boldsymbol{v}^{\text{d}}$, hence $\bar{\boldsymbol{D}} = \text{diag}\{1\ 0\ 0\ 0\}$.

The initial condition for control input ν_i with $i = 1, ..., 4$ were set as $\nu_i(0) = 0.01$ [m/s], the initial conditions for $\boldsymbol{\varphi}_i(0)$ are equal to zero, in the case of $\hat{\boldsymbol{v}}_i^{\text{d}}(0)$ the initial condition were obtained from $\boldsymbol{v}^{\text{d}}(t)$ in the instant zero, the gains proposed were set as $c = 1$, $\lambda_i = k_{\varphi i} = 2$ and $\mu = 10.5$, the constants $\boldsymbol{\delta}_i$ are $\boldsymbol{\delta}_1 = [-0.1 \ 0.1]^\top$ [m], $\boldsymbol{\delta}_2 = [0.1 \ 0.1]^\top$ [m], $\boldsymbol{\delta}_3 = [-0.1 \ -0.1]^\top$ [m] and $\boldsymbol{\delta}_1 = [0.1 \ -0.1]^\top$ [m].

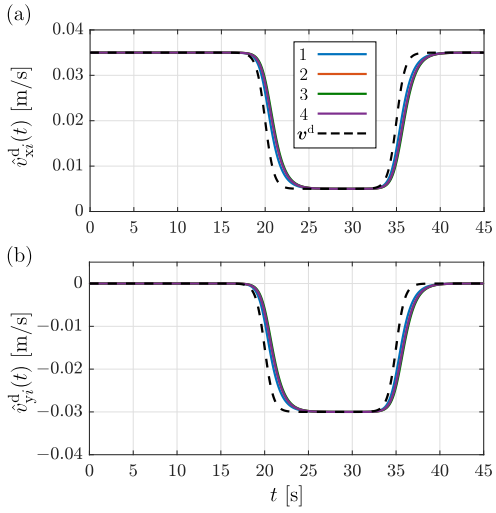

Fig. 3. Estimated velocity: (a) axis x and (b) axis y

To demonstrate that the distributed observer has a good performance in Figure 3 can be seen that the estimated desired velocity of each agent tends to the desired velocity profile even when just one agent knows it. Figure 4 shows the trajectory produced for the agent when tracking the estimated velocity profile, of this result can be also observed that the robots have achieved the desired pattern established for the constant $\boldsymbol{\delta}_i$.

To validate the aforementioned in Figure 5 can be observed that the relative position error measurements converge to zero after of the transient time, for this reason we can conclude that the robots have reached the desired formation.

 https://doi.org/10.58571/CNCA.AMCA.2025.064

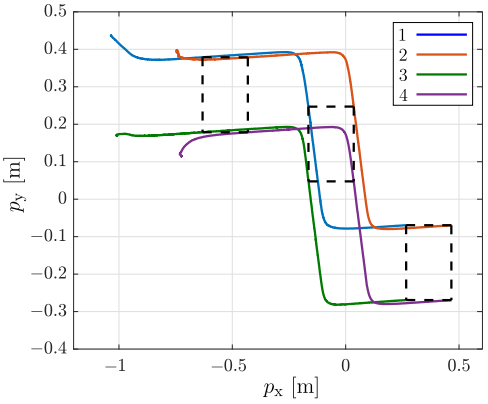

Fig. 4. Generated trajectory for the agents and desired formation

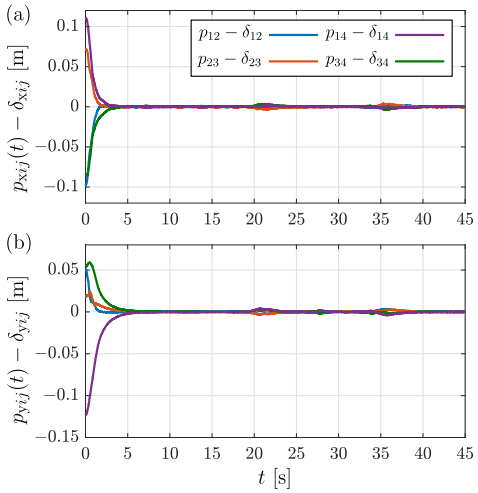

Fig. 5. Time evolution of relative position error: (a) axis x and (b) axis y

For purposes of comparison the linear velocity of the robots has been calculated using the kinematic model (2a), as can be observed in the Figure 6 the linear velocity measurements converge to the estimate desired velocities, then considering this result and the shown in Figure 5 the control objectives proposed in (1) have been accomplished, now considering that the robots also maintain the same attitude Figure 7 the flocking behavior in the sense of the established for Craig Reynolds is achieved.

The control inputs required to achieve the control objective are depicted in Figure 8, in the case of the control input ν_i (see Figure 8(a)) there is no zero-crossings, therefor, there are no indeterminations in the control input ω_i (see Figure 8(b)).

5. CONCLUSIONS

The problem of flocking was addressed in this work, to solve the problem a control law and a distributed observer were designed employing theory of nonlinear control and graph. It is important to mention that the controller proposed does not require linear velocity measurements to achieve the control objective. The above is very useful in practice, given that the computational calculations are reduced and the linear velocity sometime is not available for feedback. On the other hand, the distributed observer

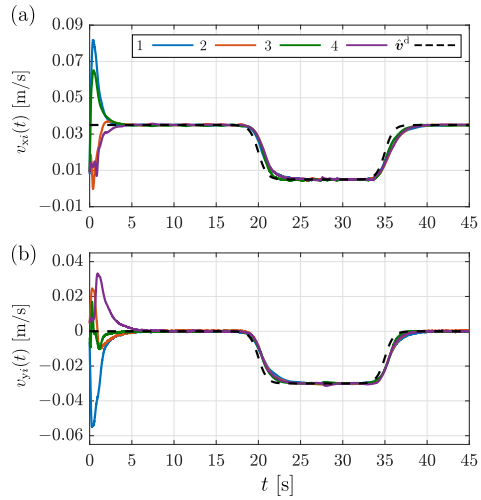

Fig. 6. Time evolution of velocity measurements of each robot: (a) axis x and (b) axis y.

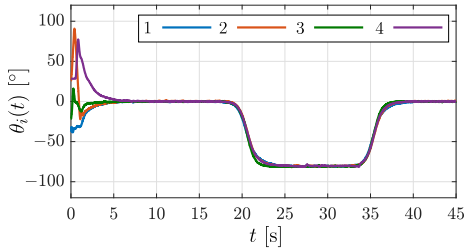

Fig. 7. Angular position of each agent

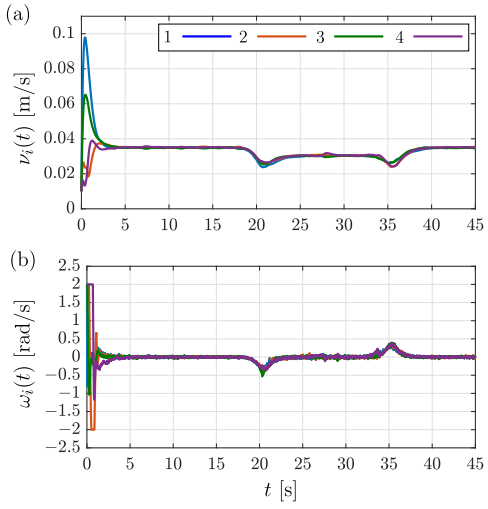

Fig. 8. Control Inputs: (a) magnitude of linear velocity and (b) angular velocity.

allows emulating the behavior under study in a more realistic way, since, as mentioned before in real life not all the agents know the flocking velocity. Employing the theory of linear control, it was proved that the closed-loop system is exponentially asymptotically stable. Through the results shown, we conclude that the controller presents a good performance. As future research, we will study the case of obstacle avoidance and attitude estimation.

 https://doi.org/10.58571/CNCA.AMCA.2025.064

REFERENCES

Abdessameud, A. and Tayebi, A. (2009). Formation control of VTOL-UAVs. *Proceedings of the 48h IEEE Conference on Decision and Control (CDC) held jointly with 2009 28th Chinese Control Conference*. doi: 10.1109/CDC.2009.5400941.

Abdessameud, A. and Tayebi, A. (2013). On consensus algorithms design for double integrator dynamics. *Automatica*, 49(1), 253–260. doi: 10.1016/j.automatica.2012.08.044.

Bazoula, A. and Nemra, A. (2013). Mobile robots formation: graph-force approach. *Mediterranean Conference on Control and Automation*. doi: 10.1109/MED.2013.6608867.

Cetina, J., Pliego, J., Martínez, R., and Cruz, C. (2025). Flocking control for a swarm of nonholonomic mobile robots without attitude measurements. *International Journal of Intelligent Robotics and Applications*, 1–14. doi:https://doi.org/10.1007/s41315-025-00432-8.

Cheng, J. and Wang, B. (2020). Flocking control of mobile robots with obstacle avoidance based on simulated annealing algorithm. *Mathematical Problems in Engineering*. doi:10.1155/2020/7357464.

Gao, J., Xu, X., Ding, N., and Li, E. (2017). Flocking motion of multi-agent system by dynamic pinning control. *IET Control Theory and Applications*, 11, 714–722. doi:10.1049/iet-cta.2016.1150.

Hale, J.K. (2009). *Ordinary differential equations*. Dover Publications.

Han, Z., Wang, L., Lin, Z., and Zheng, R. (2016). Formation control with size scaling via a complex laplacian-based approach. *IEEE Transactions on Cybernetics*, 46(10), 2348–2359. doi:10.1109/TCYB.2015.2477107.

Hong, Y., Hu, J., and Gao, L. (2006). Tracking control for multi-agent consensus with an active leader and variable topology. *Automatica*, 42(7), 1177–1182. doi: 10.1016/j.automatica.2006.02.013.

Hu, J. and Lin, Y. (2010). Consensus control for multi-agent systems with double-integrator dynamics and time delays. *IET Control Theory & Applications*, 4(1). doi:10.1049/iet-cta.2008.0479.

Jian, D., Haibo, J., Yeqiu, L., Kun, L., and Chenhui, Y. (2018). Flocking control of multi-quadrotor system of systems. In *2018 IEEE CSAA Guidance, Navigation and Control Conference (CGNCC)*, 1–6. doi: 10.1109/GNCC42960.2018.9019130.

Khaledyan, M., Liu, T., Fernandez, V., and de Queiroz, M. (2020). Flocking and target interception control for formations of nonholonomic kinematic agents. *IEEE Transactions on Control Systems Technology*, 28(4), 1603–1610. doi:10.1109/TCST.2019.2914994.

Montañez, C., Pliego, J., Arellano, A., and Cruz, C. (2023). Velocity and position tracking controllers for wheeled mobile robots. *IFAC*, 56(2), 2158–2163. doi: https://doi.org/10.1016/j.ifacol.2023.10.1121.

Montañez, C., Pliego, J., and Cruz, C. (2022). Formation control for robot networks with double integrator dynamics. In *2022 IEEE Conference on Control Technology and Applications (CCTA)*, 589–594. doi: 10.1109/CCTA49430.2022.9966124.

Moshtagh, N., Jadbabaie, A., and Daniilidis, K. (2005). Distributed geodesic control laws for flocking of nonholonomic agents. *IEEE Conference on Decision and Control*. doi:10.1109/CDC.2005.1582593.

Ning, B., Han, Q., Zuo, Z., Jin, J., and Zheng, J. (2018). Collective behaviors of mobile robots beyond the nearest neighbor rules with switching topology. *IEEE Transactions on Cybernetics*, 48(5). doi: 10.1109/TCYB.2017.2708321.

Nuño, E., Ortega, R., Basañez, L., and Hill, D. (2011). Synchronization of networks of nonidentical euler-lagrange systems with uncertain parameters and communication delays. *IEEE Transactions on Automatic Control*, 56(4), 935–941. doi: 10.1109/TAC.2010.2103415.

Oriolo, G., Luca, A.D., and Vendittelli, M. (2002). Wmr control via dynamic feedback linearization: design, implementation, and experimental validation. *IEEE Transactions on control systems technology*, 10(6), 835–852. doi:10.1109/TCST.2002.804116.

Pliego, J., Martínez, R., Cruz, C., Avilés, J., and Flores, J. (2023). Flocking and formation control for a group of nonholonomic wheeled mobile robots. *Cogent Engineering*, 10(1), 2167566. doi: https://doi.org/10.1080/23311916.2023.2167566.

Ren, W. (2008). On consensus algorithms for double-integrator dynamics. *IEEE Transactions on Automatic Control*, 53(6), 1503–1509. doi: 10.1109/TAC.2008.924961.

Ren, W., Beard, R.W., and Atkins, E.M. (2007). Information consensus in multivehicle cooperative control. *IEEE Control Systems Magazine*, 27(2), 71–82. doi: 10.1109/MCS.2007.338264.

Reynolds, C.W. (1998). *Flocks, herds, and schools: a distributed behavioral model*, 273–282. doi: 10.1145/280811.281008.

Rojo, E., Garcia, O., Ollervides, E., Zambrano, P., and Espinoza, E. (2019). Robust consensus-based formation flight for multiple quadrotors. *Journal of Intelligent & Robotic Systems*, 213–226. doi:10.1007/s10846-018-0843-3.

Saif, O., Fantoni, I., and Zavala-Río, A. (2019). Distributed integral control of multiple uavs: precise flocking and navigation. *IET Control Theory & Applications*, 13(13), 2008–2017. doi:https://doi.org/10.1049/iet-cta.2018.5684.

Scardovi, L., Arcak, M., and Sontang, E. (2010). Synchronization of interconnected systems with applications to biochemical networks: an input-output approach. *IEEE Transactions on Automatic Control*, 55(6), 1367–1379. doi:10.1109/TAC.2010.2041974.

Shi, H., Wang, L., and Chu, T. (2009). Flocking of multi-agent systems with a dynamic virtual leader. *International Journal of Control*, 82(1), 43–58. doi: 10.1080/00207170801983091.

Zhao, S. and Zelazo, D. (2017). Translational and scaling formation maneuver control via a bearing-based approach. *IEEE Transactions on Control of Network Systems*, 4(3), 429–438. doi:10.1109/TCNS.2015.2507547.

Zhao, X.W., Guan, Z.H., Li, J., Zhang, X.H., and Chen, C.Y. (2017). Flocking of multi-agent nonholonomic systems with unknown leader dynamics and relative measurements. *International Journal of Robust and Nonlinear Control*, 27(17), 3685–3702. doi: https://doi.org/10.1002/rnc.3762.

 https://doi.org/10.58571/CNCA.AMCA.2025.064